

Received January 21, 2020, accepted February 27, 2020, date of publication March 6, 2020, date of current version March 17, 2020.

Digital Object Identifier 10.1109/ACCESS.2020.2979080

RFID Based Non-Contact Human Activity Detection Exploiting Cross Polarization

XUANKE HE^{1,2}, (Student Member, IEEE), JIANG ZHU¹, (Senior Member, IEEE),
WENJING SU¹, (Member, IEEE), AND MANOS M. TENTZERIS², (Fellow, IEEE)

¹Google LLC, Mountain View, CA 94043, USA

²Georgia Institute of Technology, Atlanta, GA 30332, USA

Corresponding author: Jiang Zhu (jiangzhu@google.com)

This work was supported by the Google Internship Program.

ABSTRACT This paper explores antenna's polarization for Radio-Frequency Identification (RFID) based non-contact human activity detection. For the first time, a cross circular polarization configuration between reader antenna and tag antenna is proposed to increase the sensing range and spatial sensitivity. Compared to conventional RFID configurations - linearly polarized (LP) tag and circularly polarized (CP) reader, a cross CP configuration can improve the signal-to-noise ratio (SNR) which leads to 230% increase in the detection area over traditional approach in our experiment. As the result of the improvement of spatial sensitivity, the proposed approach can detect subtle and small body movements at almost 4.5m from the reader, such as head movements or even respiration, which enables a low-cost, easy-to-use, non-contact and non-intrusive monitoring of the elderly and disabled peoples in places like hospitals and assisted living homes.

INDEX TERMS Activity recognition, ambient computing, assisted living, health monitoring, non-contact sensing, polarization, radio-frequency identification (RFID).

I. INTRODUCTION

Human activity monitoring grants an important role in making lives easier for everyone. As people age, their livelihood are more and more dependent on caregivers or loved ones for their well being. Ubiquitous/ambient computing can help these people achieve greater autonomy in their lives by seamlessly and naturally integrating wireless sensors and computers which greatly improves their daily efficiency. Widespread, low-cost wireless sensors can enable the ambient computing revolution and help support people and their homes in case mental or physical related disabilities precludes them from getting the help that they need.

Human activity detection is a crucial part in human activity monitoring. Traditionally, camera systems or on-body sensors, such infrared sensors or accelerometer/gyroscopes, and FMCW radar [1]–[4], have been utilized to detect human activity, however, these methods comes with drawbacks [5]–[8]. For video monitoring, extensive amount of computational power is required to process the video received, and cameras have security and privacy concerns

The associate editor coordinating the review of this manuscript and approving it for publication was Mohammad Tariqul Islam¹.

making it not suitable for ubiquitous use. Wearable sensing technologies requires that the user constantly wear them which can be seen as a hassle in some cases like sleeping or exercising. In addition, people might be forgetful or lose interest in wearing them, making it a non-reliable method for activity tracking. Radar systems are not commercially available, expensive, and thus difficult to implement for widespread use.

Radio Frequency IDentification (RFID) is a low cost platform used in many industries for inventory tracking, security and asset management. RFID systems utilizes backscattering, to communicate between a reader and multiple tags. This involves transmitting a continuous wave (CW) from the reader to the tag and the tag retransmitting a modulated signal back to the reader. RFIDs have been introduced for human activity tracking [9]–[13], and has been shown to be a promising technology in tracking a wide range of human activities. These include using wearable and on-object RFIDs [14]–[16] and also device free RFID activity recognition [11], [17]. By collecting the RSSI and phase information of the tag readings, activities can be classified based on the characteristics of those readings. However, the spatial sensitivity, maximum distance which activities can be detected, is inadequate

as the human user needs to be close or in the line of sight between the RFID tag and reader in order for the activities to be detected. This is not sufficient as it results in a limited detection area, making it impractical in most real use cases. Previous works have tried to mitigate this by adding more tags [11], [13], allowing for a broader coverage area, however this becomes a hassle as the user has to manually space out multiple tags to avoid mutually coupling to each other [18], and adds general complexity. By reducing the number of tags and have each tag cover a wider area, the practicality of the system is drastically increased.

All of these works utilize commercially available RFID tags, which are linearly polarized, while most RFID readers are circularly polarized. This setup allows the RFID reader to read LP tags at any orientation, since circularly polarized electromagnetic waves can interrogate LP antennas, which makes it advantageous in places like a warehouse where products might be placed in different orientations. It might be advantageous for inventory tracking, but not for human activity tracking. To increase the spatial sensitivity, and to decrease the amount of tags required, in sensing human activity, a new approach was developed by exploiting the circularly cross polarization of the reader and tag. Understanding that electromagnetic waves changes polarization when reflected, it is possible to create a system with greater spatial sensitivity, while still utilizing the same low-cost RFID platform. This is done using a hardware level approach utilizing circularly cross polarized RFID antenna and tag.

The remainder of the paper is as follows. Section II describes the theory about why cross polarized CP tags can increase the spatial sensitivity and range and provides measurement results which validates the theory. Section III describes the design of the hardware, CP tag, and the setup of the system and calibration of the environment. Measurement results of different human activities in a typical room environment are shown in Section IV. Conclusions and future works are discussed in the final section.

II. THEORY

We exploit cross polarization between RFID reader antenna and tag antenna to improve the detection sensitivity and range of human activities. In a conventional RFID based ranging system, the magnitude (in the form of received signal strength indicator, or RSSI) and phase of the back-scattering wave from the RFID tag to the reader, are recorded to extract the tag's location. Many RFID based human activity detection systems use an on-body approach [14] where the tag is attached to the body. This approach has the benefits of larger monitoring area and higher sensitivity due to approximate to the human body, and can even detect the complex body movements when multiple tags are deployed on different parts of the body. However, on-body approach leads to many drawbacks, primarily because they need to be comfortable to wear and need to be remembered to be worn, which makes them undesired for long-term monitoring. The alternative refers to the tag-free, also referred as off-body approach, where

TABLE 1. LOS back-scattering wave – “noise” suppression versus reader-tag polarization configuration in RFID based human activity detection (V. LP refers to vertically linearly polarized and H. LP refers to horizontally linearly polarized).

| | LHCP | RHCP | V. LP | H. LP |
|-------|---------|---------|---------|---------|
| LHCP | 0 dB | > 30 dB | 6 dB | 6 dB |
| RHCP | > 30 dB | 0 dB | 6 dB | 6 dB |
| V. LP | 6 dB | 6 dB | 0 dB | > 30 dB |
| H. LP | 6 dB | 6 dB | > 30 dB | 0 dB |

the tag's location is fixed, for example, tags are mounted on the wall, and thus the change in RSSI and phase of back-scattered wave is due to the dynamic body movements in a static environment. In most of these works, the line-of-sight (LOS) signal that is directly back-scattered by RFID tags is the dominant contributor to the received signal, as the reflection is usually much weaker due to the reflection loss at the reflecting surface and larger path loss from a longer traveling distance, which agrees with the observation that if the human activity occurs far from the the line between the tag and the reader, the associated change in RSSI or phase is significantly smaller than LOS signal, which limits the detection range and the sensitivity to sense subtle body movement. The idea to deploy multiple closely-spaced tags has been proposed to address this challenge [11], [13]. However, this approach inevitably increases the cost on tags and computational load for the system.

Our proposed approach focuses on the suppression of the noise in order to improve the signal-to-noise ratio (SNR) in the RFID based non-contact system for human activity detection. Here, the “signal” is the wave reflected by human body which carries the body movement information, while the “noise” is the LOS back-scattering wave from the tag. We purposely cross-polarize the reader antenna and tag antenna as shown in Table. 1. Cross polarization refers to the electric field polarization of two signals/antennas being orthogonal to each other. Co-polarization refers to the fields being parallel. Due to the fields being perpendicular to each other, the electric fields do not align resulting in no power transmission, while co-polarization means maximum power transmission. Cross polarization can usually degrade the LOS signal strength by more than 30 dB which is referred as polarization mismatch loss. This is further verified in Section III. Therefore, the received LOS back-scattering wave as “noise” is sufficiently suppressed by utilizing cross polarized reader and tag combination. This is illustrated in Fig. 1.

We further discuss the off-body reflected “signal” in the cross circular polarization configuration which carries the information about human movements. It is known that circularly polarized electromagnetic waves when incident on a dielectric or metal surface changes the handedness of the polarization of the reflected wave [19]. For example, right-hand circular polarized (RHCP) waves which are reflected, become left-hand circular polarized waves (LHCP)

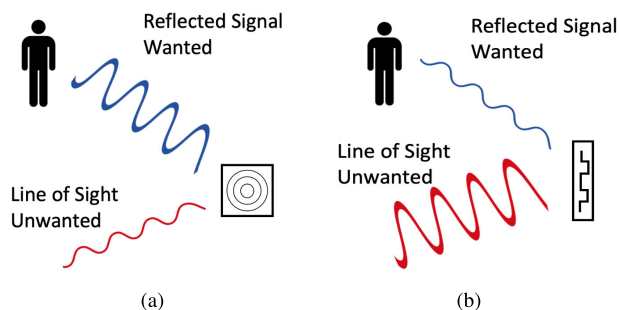


FIGURE 1. Illustration of how the signal-to-noise ratio of a RFID-based human detecting system is improved over cross circular polarization scheme as shown in (a), as compared to the traditional linear-tag approach as shown in (b).

and vice-versa. Since human tissues, such as muscle and skin, are conductive and have high relative permittivity [20], a significant amount of RF energy is reflected and this reflected signal is flipped to the cross polarized handedness to that of the incident wave. This phenomenon has been used in the miniaturization of Doppler radar for monitoring human vital signs, i.e., respiration and heartbeat [4]. In the RFID based human activity detection application, the “signal” that correlates to the human activities is not suppressed by the cross polarization configuration as whenever the interaction with human body occurs, the handedness of the reflected CP wave is flipped to the co-polarization configuration to the receiving antenna, so there is no polarization mismatch loss for the “signal”.

Several other polarization configurations between reader and tag antennas are discussed as compared to cross CP configuration. With respect to the cross LP reader and LP tag combination, the signal reflected by the body cannot be detected, because the LP wave reflection off the body makes no guarantee that the reflected wave changes its polarization, for example, from vertical linear polarization to horizontal linear polarization [21]. In the case of co-polarized CP reader and tag combination, the reflected wave due to the body has the opposite handedness to the reader or tag, which results in large polarization mismatch loss to the “signal” while enhancing the LOS back scattering wave directly from the tag as “noise”, which leads to the least preferred configuration for the tag-free human activity detection application as the result of poor SNR. For all other reader and tag combinations, the reflected signal is not degraded by cross polarization mismatches, aside from the 6 dB which arises from LP to CP polarization loss. The result is summarized in Table. 2. By comparing the two tables, when overlaid with each other, it can be seen that RHCP and LHCP combination, the two cross circular polarization combinations, can suppress the LOS and enhance the body reflection signal.

To prove the theory, a linear polarized tag and a LHCP tag were measured using a RHCP polarized RFID reader in an anechoic chamber. The details about circular polarized RFID tag design are given in Section III. In this experiment, the reader and tags were separated by 1.5 meters with antenna’s peak gain aligned at LOS. RSSI was recorded

TABLE 2. Reflected wave – “signal” degradation versus reader-tag polarization configuration in RFID based human activity detection (V. LP refers to vertically linearly polarized and H. LP refers to horizontally linearly polarized).

| | LHCP | RHCP | V. LP | H. LP |
|-------|---------|---------|---------|---------|
| LHCP | > 30 dB | 0 dB | 6 dB | 6 dB |
| RHCP | 0 dB | > 30 dB | 6 dB | 6 dB |
| V. LP | 6 dB | 6 dB | 0 dB | > 30 dB |
| H. LP | 6 dB | 6 dB | > 30 dB | 0 dB |

with and without reflective objects, i.e., human or human-sized metallic sheet as shown in Fig. 2. On the one hand, when there is no reflective object inside the chamber which is referred as “Empty” scenario, the RSSI level for LHCP tag is as low as close to the sensitivity level of the RFID reader around -70 dBm as shown in 2 (c) which is at least 15 dB lower than that of linear tag measured under the same condition shown in 2 (d), because the link maintains only through the LOS back-scattering path. With the polarization mismatching between the reader antenna and the tag antenna, the back-scattering link of LHCP tag even dropped at higher frequencies over 915 MHz. On the other hand, when a human or metallic sheet was presented in the chamber, the reflection path was created. The measured RSSI with LHCP tag is increased by in the order of 10 dB and 20 dB for the presence of human body and metal sheet, respectively, as compared against only 1 dB and 2 dB RSSI increase for linear tag. It is expected that the RSSI variation with the presence of metal sheet is larger than human body because the reflection loss from a perfect conductor is negligible. These experiments verify that LHCP-RHCP configuration in RFID system can effectively suppress the LOS signal strength while enabling the reception of the reflected signal. This result also shows that the CP tags are much more sensitive to human presence, given their large variations in RSSI compared to the LP tags, which suggests that the cross circular polarization configuration can enable the small and subtle body movement detection that is barely possible for LP tags.

III. DESIGN AND SETUP

The proposed RFID based non-contact human activity detection system consists of one regular RFID reader and a circular polarized RFID tag. The RFID reader used for measurement was the Impinj RFID R420 reader with a maximum sensitivity of -72 dBm. One LHCP reader (S9028PC) antenna was utilized in this paper, with 9dBi of gain. The RFID reader was connected to a PC running a Java program written using the Impinj Octane SDK. When reading tags, the RFID reader outputs a stream of objects which includes information on the tag such as its individual product code, RSSI, phase and timestamp. In this paper, the RFID reader operated in the MAXTHROUGHPUT mode, which gives around 250 tag reads per second, or one tag read every 4 ms and operated at 31.5 dBm output power. In this mode, the read frequency

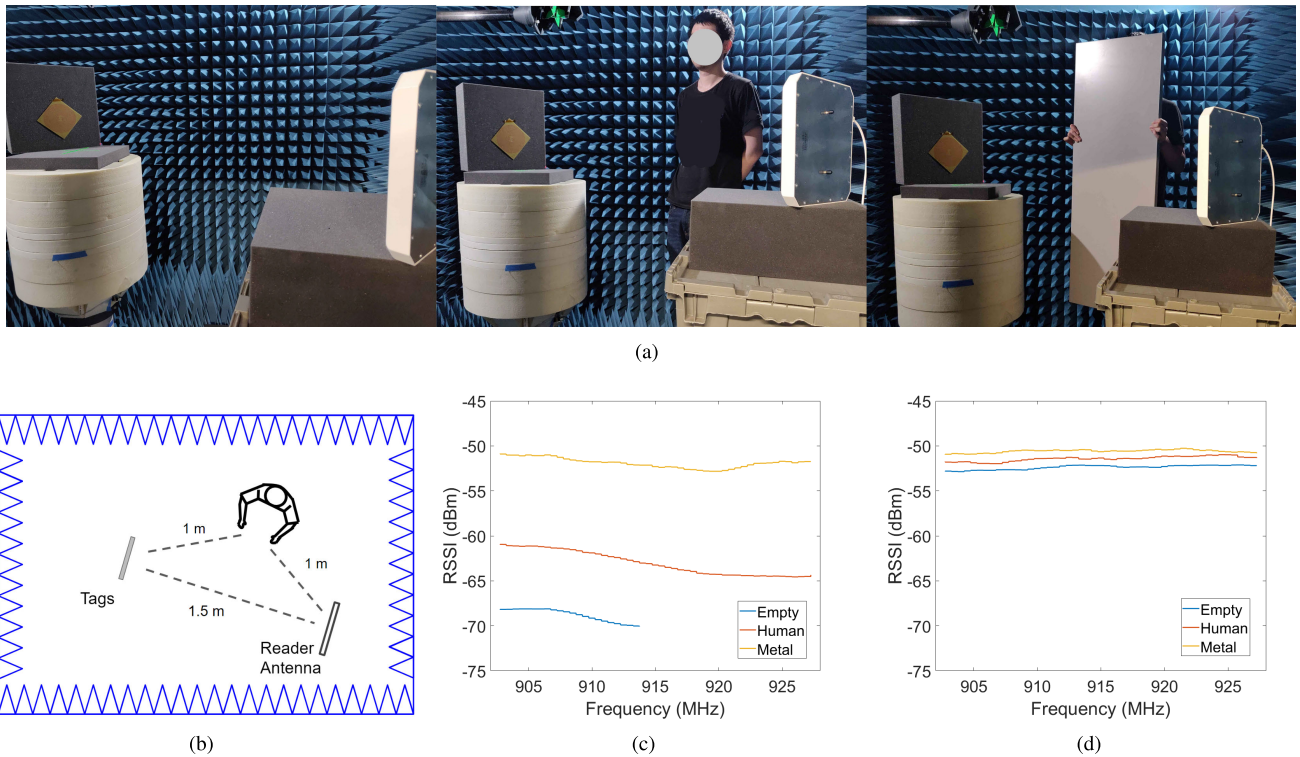


FIGURE 2. (a) Human multi-path reflection sensitivity test with 3 conditions, empty chamber, human inside chamber and human sized metal sheet. The experiment was repeated for both LP and CP tags. (b) Layout inside the chamber. (c) Different environment's effects on RSSI of CP tag. In an empty chamber, at frequencies >915 MHz, the RSSI cannot even be measured because it is lower than the reader's sensitivity (d) Different environment's effects on RSSI of LP tag. In the case of the CP tag, a dramatic increase was measured in the RSSI due to the introduction of reflectors.

can detect just about every human gesture. A typical linearly polarized tag, SmartTrac BELT R6, which measures $70 \text{ mm} \times 10 \text{ mm}$, with an Impinj Monza R6 RFID chip was utilized as a comparison to the custom designed circularly polarized RFID tag.

A. CIRCULAR RFID TAG DESIGN

Since the majority of the commercially-off-the-shelf tags are linearly polarized, a circularly polarized tag was custom-designed for our study. Spiral antennas are a common class of antennas which are frequency independent [22], meaning that its characteristics, such as antenna pattern, bandwidth and polarization remains unchanged with respect to frequency. This makes the spiral antenna the ideal candidate for the circularly polarized tag, as the only remaining parameter to design is a matching network between the RFID chip to the antenna. The RFID chip used on the circularly polarized tag is the same Impinj Monza R6 chip (Murata LXMS21ACMF-183) as on the SmartTrac LP tag. To obtain maximum power transfer from the tag antenna to the chip, a conjugate match must be designed so that the reactance of the chip is cancelled by the reactance of the antenna, so that the antenna only sees a real impedance load. This is done by utilizing a T-shaped matching network feed [23] where both arms of the archimedes spiral symmetrically extend outwards from, which matches the $20\text{-}145j \ \Omega$ impedance of the chip

its complex conjugate impedance. The tag was fabricated on 0.8mm thick FR4, to maintain a low cost and lightweight tag, and has a radius of 13 cm. The antenna simulation and fabricated model is shown in Fig. 3 (a) and (b), and simulated results in (c)-(e), with a realized gain of 3.3 dBi and axial ratio bandwidth of 105 degrees. In addition, the SmartTrac Belt RFID tag was also modeled in simulation, which has only 0.3 dB of simulated realized gain, to serve as a comparison for the CP tag.

The characterization of the proposed spiral CP tags was conducted in an anechoic chamber environment to reduce interference and to remove any unwanted multi-path effects. To gauge the performance, RSSI is measured with a co-polarized reader mounted inside an anechoic chamber. A comparison with a conventional linear polarized tag is made by replacing the CP tag with the LP tag at the same location. The measured RSSI readings are shown in Fig. 4, which shows that the CP tag in co-polarized mode, has around 13 dBm better RSSI than the linear tag. This makes sense as the CP tag has 3 dB difference in gain and 3 dB polarization matching. With twice the link budget, due to the nature of back-scattering as the tag both transmits and receives, this is an expected 12 dB increase in RSSI, similar to prediction. Additionally, as compared to Fig. 3 (c) in the "Empty" chamber case, the cross polarization loss of the tag to the reader antenna is greater than 30 dB. This demonstrates that

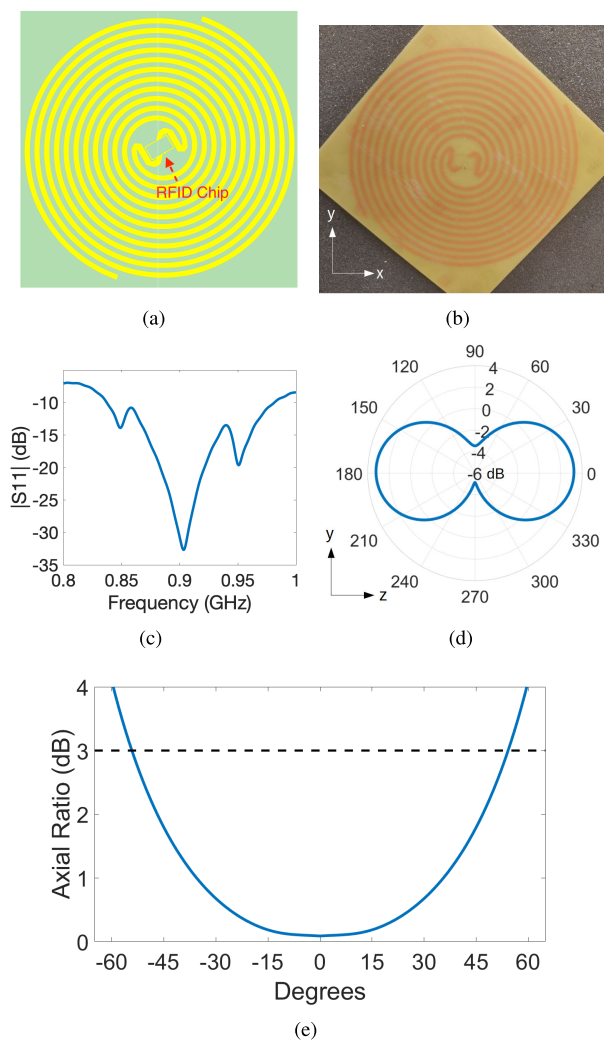


FIGURE 3. (a) CP tag CAD model. (b) Fabricated CP tag. (c) S11 of the tag showing < -10 dB matching across the RFID band. (d) Gain pattern of the tag with 3.3 dB simulated gain. (e) Axial ratio plot of the CP tag at 915 MHz cut along the broadside, showing around 105 degrees of axial ratio bandwidth.

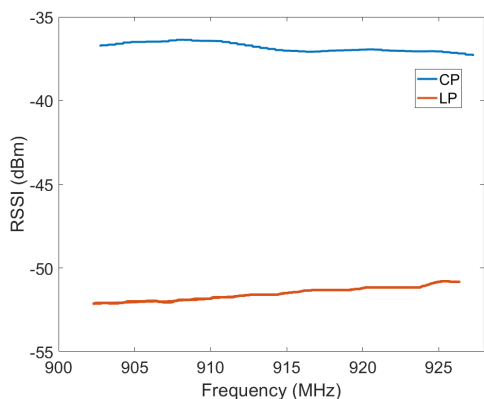


FIGURE 4. Tag comparison between LP and CP tags, showing around 13 dBm increase in RSSI, verifying that the CP antenna operates correctly.

the CP tag’s matching and polarization also matches closely with the calculation, verifying that the CP tag operates as designed.

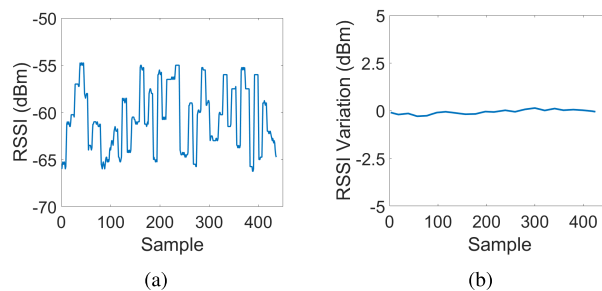


FIGURE 5. Demonstration of the frequency hopping calibration of the RFID reader. (a) Pre-calibration, showing the individual hops that the RFID reader goes through. It is noted that the RSSI only changes when the reader hops frequency. The phase (not shown) also demonstrates similar behavior. (b) Post-calibration. If there is no movement, when referenced to the calibration data, the variation is 0.

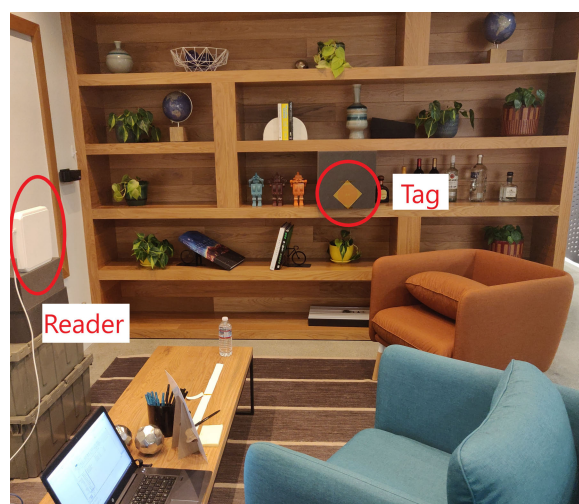


FIGURE 6. Typical room environment for testing with the tag and reader antenna close to the walls.

B. DATA PRE-PROCESSING

RFID system requires a reader to collect the back-scattered tag information, which can extract the RSSI and phase information of the tags from the backscattered signal. It is observed that the Impinj R420 RFID reader uses frequency hopping spread spectrum transmission technique meaning that the reader hops through the 50 channels within the allocated 902-928 MHz frequency band every 10 seconds. This is an unchangeable feature within the reader, which reduces interference between multiple readers. In most real use cases, multi-path has a large variation on the both the RSSI and phase information, making it difficult to extract any information from the collected data as seen in Fig. 5 (a). However, the RSSI and phase readings are constant for the fixed environment. Thus, it is possible to utilize the tag to obtain a calibration of the room before anything has moved, and observe the effect of the object moving on the RSSI or phase relative to the calibration data. To calibrate the environment, first a 10 second measurement is conducted to ensure that the Impinj R420 hops through all 50 channels, and the RSSI and phase data is saved for each of the 50 frequencies.

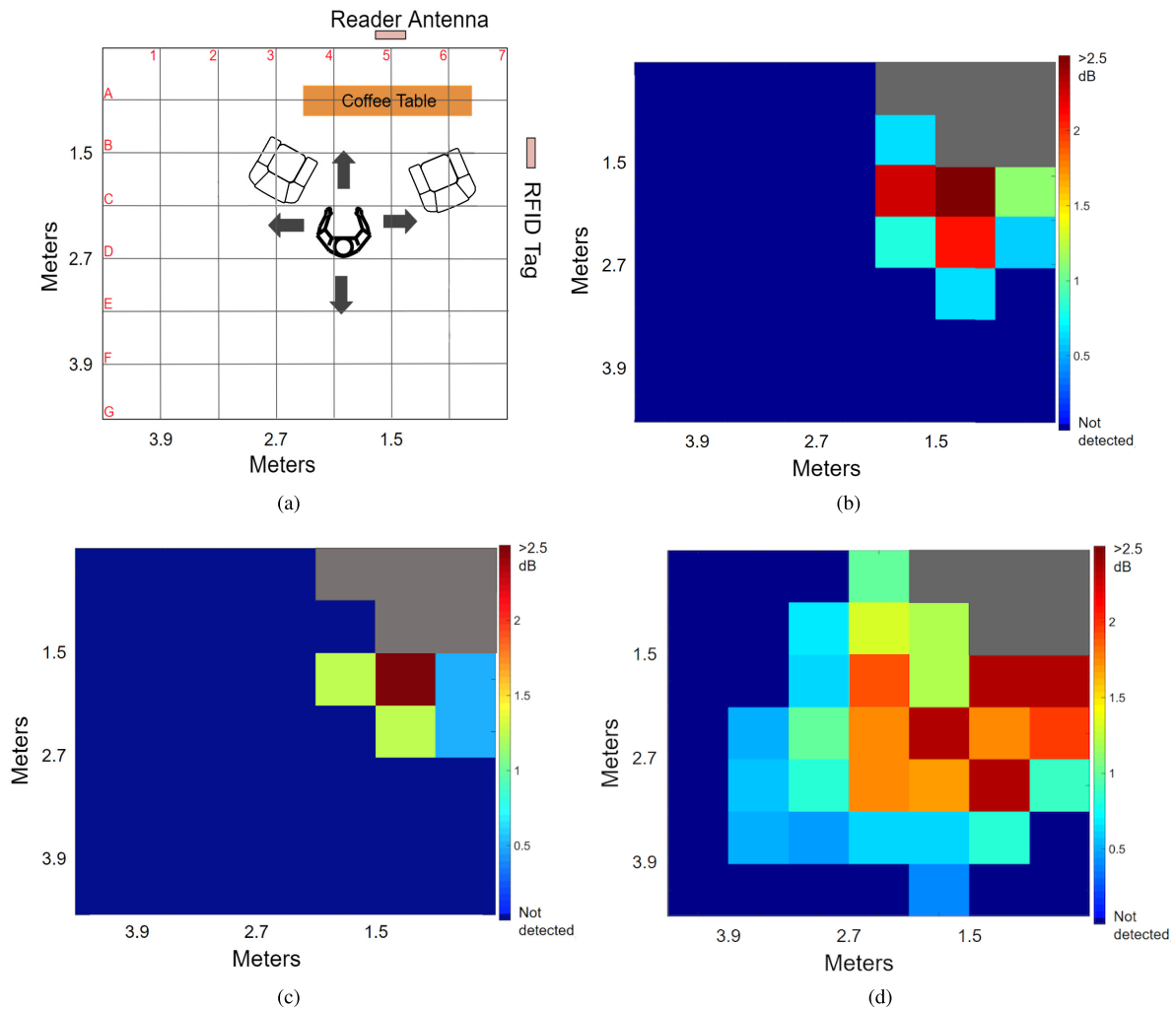


FIGURE 7. (a) Layout of the testing area, each block measuring an area around 60cm × 60 cm. The grid starts 30 cm away from the tag and reader. (b) Vertically oriented LP tag detection heatmap. (c) Horizontally oriented LP tag detection heatmap. (d) Cross polarized CP tag detection heatmap. The scale measures the RSSI variations in terms of dB. The point directly in front of the both the tag and reader generates the largest variations.

To calibrate the RSSI, a 10-seconds long RSSI data is saved in key-value pairs, with value being the mean of the RSSI values collected withing a channel and the key being the frequency channel. During measurements, the collected RSSI data of the RSSI, is referenced to the original saved calibration data by simple subtraction to find the difference between the calibrated and measured. For phase measurements, the method in [24] is implemented, shown in Equation 1:

$$\theta_c = \left[\frac{f_j}{f_i} \times (\theta_{d,i} - \theta_{d_0,i}) + \theta_{d_0,j} \right] \text{mod } 2\pi \quad (1)$$

where the fixed frequency is denoted as f_j and the current measured frequency channel is f_i . $\theta_{d,i}$ and $\theta_{d_0,j}$ denotes the saved phase data for channels i and j and $\theta_{d_0,j}$ denotes the current measured tag phase at channel j . In this method the phase measurements at different channels are remapped to a chosen fixed frequency j . The phase is remapped to a frequency which has an initial phase closest

to π to give the remapped response a wide $[0 \ 2\pi]$ range without phase wrapping.

These techniques result in a flat response without frequency hopping variations, Fig. 5 (b), to better visualize the response of human activities as variations from a baseline. By knowing the baseline data, prior to any movement, the RFID reader can detect variations in the multi-path, induced by movements or gestures by human interactions. When various activities are performed, the deviation illustrates the multi-path effects of the activity, with each unique activity affecting the multi-path differently, resulting in variations in the RSSI and phase. The preprocessing step important to data collection as the data is based on variations, Fig. 5 (b) rather than on raw data, Fig. 5 (a). This gives activities more variation and better visualization, allowing for the system to better detect when the activity is occurring and analyze its effect on RSSI and phase. When the the user performs an activity and returns to the original position, the RSSI and phase should also return to their original calibrated positions.

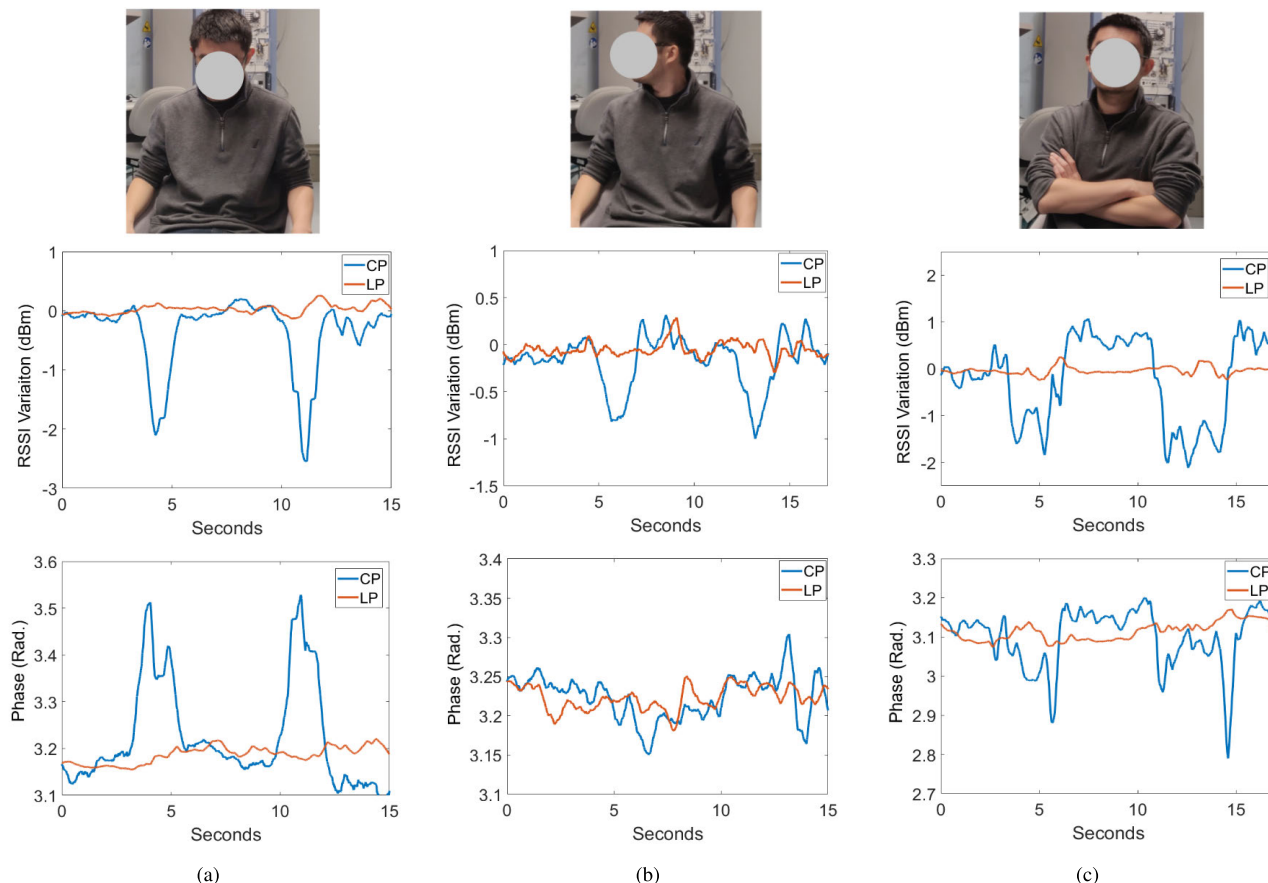


FIGURE 8. 3 activities demonstrated (top) and their RSSI variations (middle) and phase variations (bottom). Activities are repeated, then the user goes back to the original calibrated state, and two of the activities are shown in the plots. Using the CP tag increases the variations of the activities, and it is evident that most of the activities differ from each other, either in RSSI variation or phase variation. For example, the shaking head activity generates a smaller dip in RSSI compared to the other two activities, and the nodding head generates a large increase in phase while the other two do not.

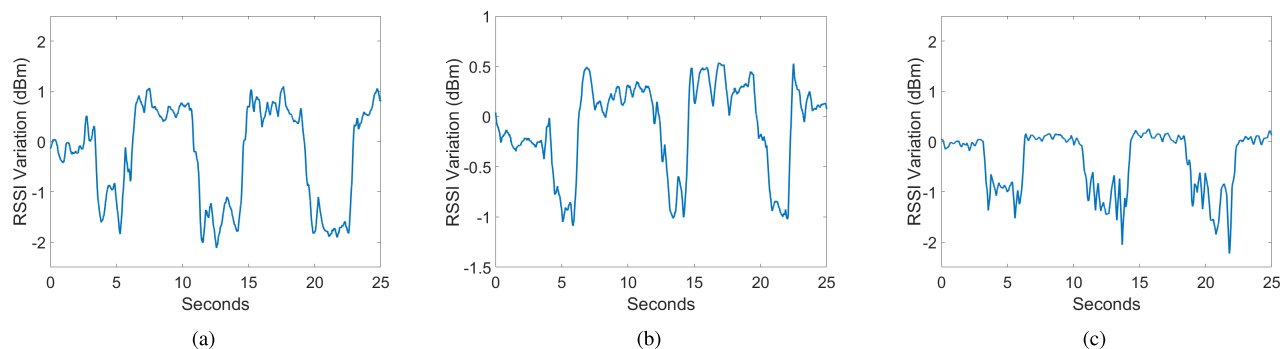


FIGURE 9. Crossing arm activity repeated for 3 different users (a), (b) and (c) and the effect of the activity on the RSSI. Different users perform actions differently, such as in speed or position, in addition to their difference in height and posture, but for all 3 users the crossing arm activity generally demonstrates a dip in the RSSI.

Using this data preprocessing method for calibrating the RSSI and phase allows the activities to be clearly and accurately detected.

IV. EXPERIMENTS

While the antenna chamber testing result demonstrates a better sensitivity from the cross CP tag than that of the LP tag, it is only evident in the electromagnetic controlled

environments. To further validate the theory, tests must be performed in the real-life environments. A typical environment is shown in Fig. 6, which consists of tables, chairs and shelves, as well as the floor, ceiling and walls of a building.

A. SPATIAL SENSITIVITY ENHANCEMENT TEST

In this test, an LHCP reader antenna (S9028PC) and the custom-designed RHCP tag, from the previous section as

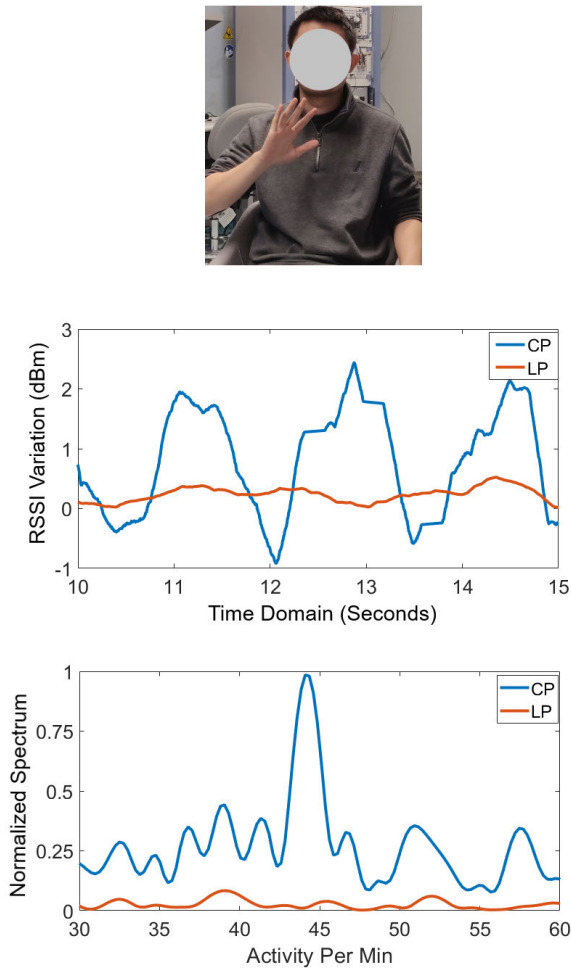


FIGURE 10. Response of the CP tag due to a repetitive activity, hand-waving. (Middle) RSSI variation at 45 waves per minute. (Bottom) FFT of the variation, demonstrating a large spike at around 45 activities per minute. However the linear tag did not experience large variations.

shown in Fig. 3 (b), are placed on opposing walls 1.5 meters away from a corner along the walls. The tag is mounted on walls to be unobtrusive and save the space. Both the tag and the antenna are 1.2 m above the floor. To verify that the CP tag has better spatial sensitivity compared to traditional linear tags, an experiment was performed on the user with identical activities, i.e., nodding their head up and down. The comparison of RSSI change was made between the CP tag and LP tag at various locations around the room for the same gesture from the user. The RSSI variation must be identifiable that is correlated to the body movement to avoid to be considered as noise. A simple sliding window algorithm was implemented. If the mean value of the sliding window reaches above a certain threshold for a period of 5 shifts, the activity is recorded, and the largest variation is measured. The window size is 10 which averages 40 ms of data and the threshold was set to be 0.3 dB. The experiment was repeated for the linear tags in both horizontal (parallel to the floor) and vertical (perpendicular to the floor) orientations for the

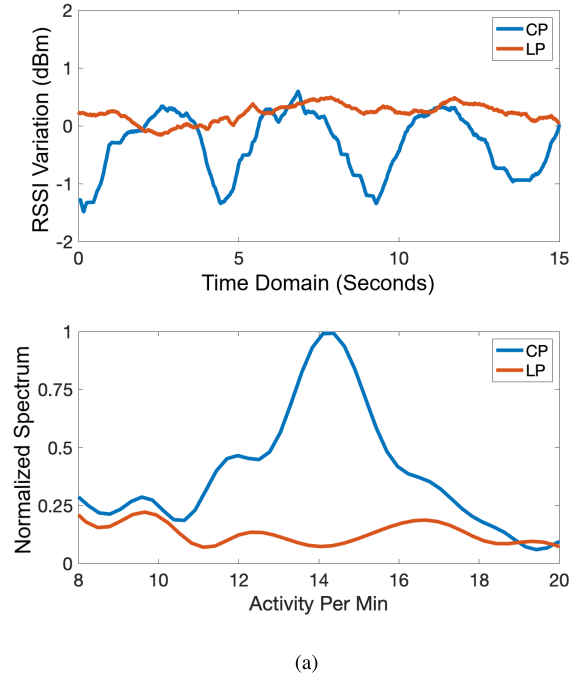


FIGURE 11. Respiration data shows drastic improvements due to the CP tag as compared to LP tag. This data was recorded at location C6.

completeness of the linear tag comparison with the CP tag. At each location the nodding head activity was repeated every 7 seconds over 1 minute long time window. The area between the tag and the reader antenna were not measured since those were in the line of sight of each other. Their heatmaps are plotted in Fig. 7. It can be observed that a single CP tag can cover and detect small body motions, in a large room, which is over 230% increase in the coverage area, due to its better sensitivity to body motions over the LP tag. It is also noted that the vertically linear polarized tag has slightly better spatial sensitivity than a horizontally LP tag. This is because the “donut”-shaped radiation pattern from a LP tag results in a better radiation coverage across all angles on the plane that is parallel to the floor, when the tag is vertically placed than horizontally placed.

B. NON-REPETITIVE ACTIVITIES

A variety of activities were performed to provide verification that the CP tag can be utilized in more than just one activity. These are classified as non-repetitive because they are usually only performed once or twice. The vertically polarized linear tag is used throughout the rest of the experiments because it performs better than the horizontally polarized tag in spatial sensitivity than the horizontally placed tag. Nodding head, shaking head, and hand-waving were 3 other activities that were performed and were performed at location C4 in Fig 7 (a). These are plotted in Fig. 8. It can be seen from the plots that at the same location, any activity performed was not able to be picked up by the LP tag, but the CP tag demonstrated a large variation in the RSSI and the phase

and the patterns exhibited by the activity on the RSSI and phase can be clearly distinguishable. It is also noted that the phase of the RFID signal varies less, and is more difficult to observe when the RSSI variations are small, meaning that the RSSI response is more sensitive than the phase. Additionally, the same tests were performed on 3 different users, which shows similar trends among the different users in Fig. 9. Although different users perform activities differently, for example the speed or position of the arms, the crossing arm activity always appears to register a drop in RSSI for all 3 users.

C. REPETITIVE ACTIVITIES

Some other activities are repetitive, so they can be analyzed down to their frequency components using fast Fourier transform. We take hand-waving activity for example. The user sat at location C4 in Fig 7 (a) and performed hand-waving at the rate of 45 times per minutes. A timer is used to ensure the repeatability. The measured results of the CP tag show clear, discernable and repetitive transient hand-waving responses shown in Fig. 10 while its frequency response shows good correlation to the expected hand-waving rate. In contrast, the LP tag shows small and uncorrelated RSSI variation with respect to hand waving, and even indicates wrong hand-waving rate from the frequency response.

Respiration, another repetitive movement due to the contraction and expansion of the chest, can also be detected through our CP tag. In the experiment, the user sits at C6 position in Fig 7 (a), which is an area directly in front of the reader. This area generates the largest variations in RSSI. As shown in Fig. 11, a clear transient domain respiration pattern and 14 breaths per minute count in frequency domain are observed from the measurement with CP tag while respiration pattern can be barely retrieved from LP tag in the same plot.

From these measurement results, it is observed that the largest variations occur when the human torso is being blocked (crossing arms, waving) or moving (respiration), since the torso is the largest part of the human body. This gives further indication that the increase in sensitivity is due to the cross polarized reflected signals.

D. SIGNAL-TO-NOISE RATIO

An FFT is performed on head nodding activity in Fig. 7 to examine the signal-to-noise ratio with both LHCP-RHCP configuration and LP-RHCP configuration. Fig. 12 shows its SNR plot at various locations which correspond to different distances between the tag and the human body. The plot is normalized to the maximum peak, whether it is CP or LP. The “noise” is defined as any other peak excluding harmonics as shown in Fig. 12 (a). It is noted that at a close range, i.e., location C5, the frequency responses between LP and CP tags are similar as shown in Fig. 12 (c). However, the signal level of the LP signal at a further range, i.e., location G1, is degraded to the noise level that can be seen from Fig. 12 (a).

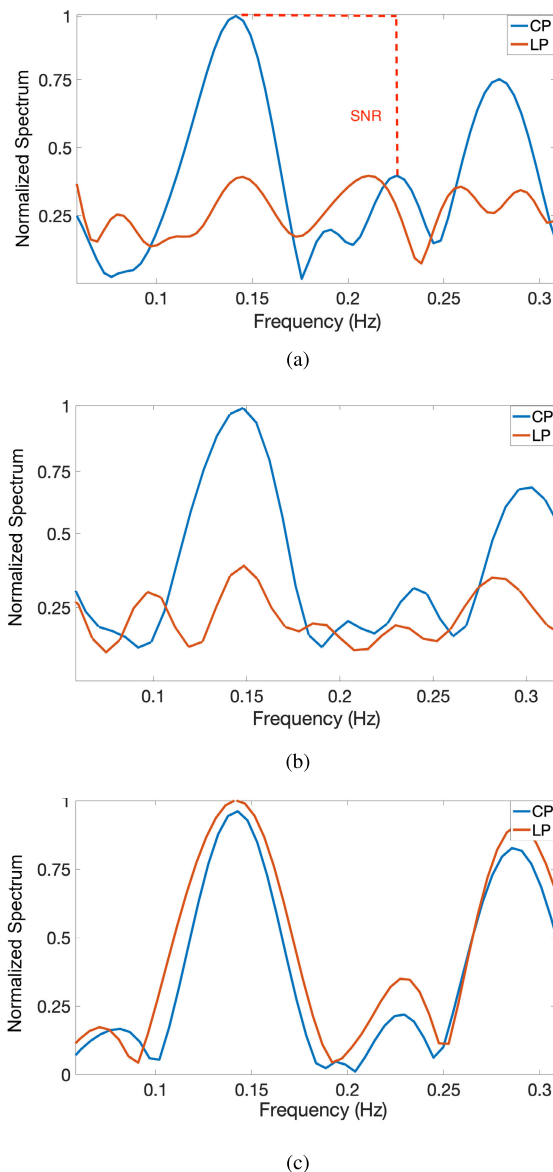


FIGURE 12. Measured frequency spectrum of the nodding head activity. Each activity, head nodding, was conducted at around once every 7 seconds, which introduces a large peak at around 0.14Hz. The second peak is due to harmonics of the signal at around 0.28 Hz. Measurement at (a) G1 (b) E3, (c) C5 location as defined in Fig. 7 (a). Since G1 is farthest from both the reader and the antenna, the peak for the LP tag readings is not discernable from noise. But at (a), the peaks at 0.14Hz is discernable. The SNR is defined as the ratio between the main peak and any other peaks excluding the harmonics.

This demonstrates that the cross CP tag has superior SNR performance with an extended range and can even detect body motions that are hidden behind noise better than their LP counterparts.

By exploiting cross polarization between reader and tag antennas in a RFID based non-contact sensing system, the RSSI and phase information can be obtained with a significantly improved signal-to-noise ratio, allowing the system to classify human activities at a further distance or at a smaller body movement scale like respiration. With the aid of

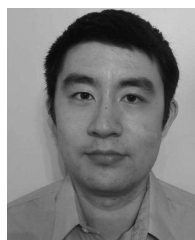
machine learning, more unique features from cross polarized RFID system can be used to better train a model and improve the accuracy of human activity recognition.

V. CONCLUSION

We discuss how the polarization configuration between reader antenna and tag antenna affects the performance of a RFID based non-contact human activity detection system. For the first time, we propose to use cross circular polarization configuration to improve the signal-to-noise ratio which leads to a larger sensing range and a higher spatial sensitivity over the conventional circular reader and linear tag combination. We fabricated spiral circular polarized RFID tags and conducted experiments in anechoic chamber environments to verify our theory. Additional real use case experiments were conducted using various gestures and small body movements, including nodding/shaking head, waving hand and respiration, to demonstrate the effectiveness of the proposed approach. The presented work provides a low-cost and non-intrusive solution for ambient computing at home and office, and enables the healthcare solutions in hospital and other indoor environments.

REFERENCES

- [1] J. Liu, Z. Wang, L. Zhong, J. Wickramasuriya, and V. Vasudevan, "uWave: Accelerometer-based personalized gesture recognition and its applications," in *Proc. IEEE Int. Conf. Pervas. Comput. Commun.*, Mar. 2009, pp. 1–9.
- [2] Z. Ren, J. Meng, and J. Yuan, "Depth camera based hand gesture recognition and its applications in human-computer-interaction," in *Proc. 8th Int. Conf. Inf., Commun. Signal Process.*, Dec. 2011, pp. 1–5.
- [3] F. Adib, Z. Kabelac, D. Katabi, and R. C. Miller, "3D Tracking via Body Radio Reflections," in *Proc. 11th USENIX Conf. Networked Syst. Des. Implement. (NSDI)*. Berkeley, CA, USA: USENIX Association, 2014, pp. 317–329.
- [4] Y. He, C. Gu, H. Ma, J. Zhu, and G. V. Eleftheriades, "Miniaturized circularly polarized Doppler radar for human vital sign detection," *IEEE Trans. Antennas Propag.*, vol. 67, no. 11, pp. 7022–7030, Nov. 2019.
- [5] P. C. Shih, K. Han, E. Poole, M. B. Rosson, and J. Carroll, "Use and adoption challenges of wearable activity trackers," in *Proc. iConf.*, 2015, pp. 1–12.
- [6] D. Townsend, F. Knoefel, and R. Goubran, "Privacy versus autonomy: A tradeoff model for smart home monitoring technologies," in *Proc. Annu. Int. Conf. IEEE Eng. Med. Biol. Soc.*, Aug. 2011, pp. 4749–4752.
- [7] D. N. Serpanos and A. Papalambrou, "Security and privacy in distributed smart cameras," *Proc. IEEE*, vol. 96, no. 10, pp. 1678–1687, Oct. 2008.
- [8] Y. Hou, Y. Wang, and Y. Zheng, "TagBreathe: Monitor breathing with commodity RFID systems," in *Proc. IEEE 37th Int. Conf. Distrib. Comput. Syst. (ICDCS)*, Jun. 2017, pp. 404–413.
- [9] D. Zhang, J. Zhou, M. Guo, J. Cao, and T. Li, "TASA: Tag-free activity sensing using RFID tag arrays," *IEEE Trans. Parallel Distrib. Syst.*, vol. 22, no. 4, pp. 558–570, Apr. 2011.
- [10] T. Wei and X. Zhang, "Gyro in the air: Tracking 3D orientation of batteryless Internet-of-things," in *Proc. 22nd Annu. Int. Conf. Mobile Comput. Netw. (MobiCom)*. New York, NY, USA: ACM, 2016, pp. 55–68, doi: 10.1145/2973750.2973761.
- [11] L. Yao, Q. Z. Sheng, X. Li, T. Gu, M. Tan, X. Wang, S. Wang, and W. Ruan, "Compressive representation for device-free activity recognition with passive RFID signal strength," *IEEE Trans. Mobile Comput.*, vol. 17, no. 2, pp. 293–306, Feb. 2018.
- [12] D. P. Hutabarat, D. Patria, S. Budijono, and R. Saleh, "Human tracking application in a certain closed area using RFID sensors and IP camera," in *Proc. 3rd Int. Conf. Inf. Technol., Comput., Electr. Eng. (ICITACEE)*, Oct. 2016, pp. 11–16.
- [13] G. A. Oguntala, R. A. Abd-Alhameed, N. T. Ali, Y.-F. Hu, J. M. Noras, N. N. Eya, I. Elfergani, and J. Rodriguez, "SmartWall: Novel RFID-enabled ambient human activity recognition using machine learning for unobtrusive health monitoring," *IEEE Access*, vol. 7, pp. 68022–68033, 2019.
- [14] R. Bainbridge and J. A. Paradiso, "Wireless hand gesture capture through wearable passive tag sensing," in *Proc. Int. Conf. Body Sensor Netw.*, May 2011, pp. 200–204.
- [15] K. Cheng, N. Ye, R. Malekian, and R. Wang, "In-air gesture interaction: Real time hand posture recognition using passive RFID tags," *IEEE Access*, vol. 7, pp. 94460–94472, 2019.
- [16] H. Li, C. Ye, and A. P. Sample, "IDSense: A human object interaction detection system based on passive UHF RFID," in *Proc. 33rd Annu. ACM Conf. Hum. Factors Comput. Syst. (CHI)*. New York, NY, USA: ACM, 2015, pp. 2555–2564, doi: 10.1145/2702123.2702178.
- [17] W. Ruan, Q. Z. Sheng, L. Yao, T. Gu, M. Ruta, and L. Shanguan, "Device-free indoor localization and tracking through human-object interactions," in *Proc. IEEE 17th Int. Symp. A World Wireless, Mobile Multimedia Netw. (WoWMoM)*, Jun. 2016, pp. 1–9.
- [18] S. E. Asl, M. T. Ghasr, M. Zawodniok, and K. E. Robinson, "Preliminary study of mutual coupling effect on a passive RFID antenna array," in *Proc. IEEE Int. Instrum. Meas. Technol. Conf. (I2MTC)*, May 2013, pp. 138–141.
- [19] W. Swindell, "Handedness of polarization after metallic reflection of linearly polarized light," *J. Opt. Soc. Amer.*, vol. 61, no. 2, pp. 212–215, Feb. 1971. [Online]. Available: <http://www.osapublishing.org/abstract.cfm?URI=josa-61-2-212>
- [20] X. Qing, Z. Ning Chen, T. S. P. See, C. Khan Goh, and T. Meng Chiam, "Characterization of RF transmission in human body," in *Proc. IEEE Antennas Propag. Soc. Int. Symp.*, Jul. 2010, pp. 1–4.
- [21] D. Chizhik, J. Ling, and R. A. Valenzuela, "The effect of electric field polarization on indoor propagation," in *Proc. IEEE Int. Conf. Universal Pers. Commun. Conf. (ICUPC)*, vol. 1, Oct. 1998, pp. 459–462.
- [22] C. A. Balanis, *Antenna Theory: Analysis and Design*. New York, NY, USA: Wiley, 2005.
- [23] G. Marrocco, "The art of UHF RFID antenna design: Impedance-matching and size-reduction techniques," *IEEE Antennas Propag. Mag.*, vol. 50, no. 1, pp. 66–79, Feb. 2008.
- [24] Y. Wang and Y. Zheng, "Modeling RFID signal reflection for contact-free activity recognition," *Proc. ACM Interact., Mobile, Wearable Ubiquitous Technol.*, vol. 2, no. 4, pp. 193:1–193:22, Dec. 2018, doi: 10.1145/3287071.



XUANKE (TONY) HE (Student Member, IEEE) received the B.S. degree (Hons.) in electrical engineering from the Georgia Institute of Technology, Atlanta, GA, USA, in 2016, where he is currently pursuing the Ph.D. degree with the ATHENA Labs.

His research focuses on using additive manufacturing to enable low-cost scalable 5G and mm-wave electronics, packaging, antennas for applications in wireless communications, sensing, and energy harvesting. He is currently focusing on developing novel ways of utilizing additive manufacturing to further integrate microwave components into useful and cost/space saving devices.



JIANG ZHU (Senior Member, IEEE) received the B.S. degree in electrical engineering from Zhejiang University, China, in 2003, the M.A.Sc. degree in electrical engineering from McMaster University, Canada, in 2006, and the Ph.D. degree in electrical engineering from the University of Toronto, Canada, in 2010.

From 2010 to 2014, he was a Senior Hardware Engineer with Apple Inc., Cupertino, CA, USA. From 2014 to 2016, he was with Google[X] Life

Science and then Verily Life Science, a subsidiary of Alphabet Inc. He is currently with Google LLC, Mountain View, CA, USA, as an Engineering Manager of Wireless Hardware Group for emerging wearable, virtual reality and augmented reality technologies and projects. He has published scientific results in *Physical Review Letters*, the IEEE TRANSACTIONS ON ANTENNAS AND PROPAGATION, the IEEE TRANSACTIONS ON MICROWAVE THEORY AND TECHNIQUES, the IEEE ANTENNAS AND WIRELESS PROPAGATION LETTERS, and *IET Microwaves, Antennas Propagation, and Electronic Letters*. He holds over 50 granted/filed US patents. His research interests include antennas, wearables, the Internet of Things, and wireless sensing. He is a member of the IEEE AP-S Industrial Initiatives and Listings Committee and the IEEE MTT-26 RFID, Wireless Sensors and IoT Committee. He serves on TPC and TPRC for numerous conferences, including the IEEE APS, IMS, and RWS. He was a recipient of the IEEE Microwave Theory and Techniques Society Outstanding Young Engineer Award, in 2020, and the IEEE Antennas and Propagation Society Doctoral Research Award, in 2009. He was an Associate Editor of the IEEE INTERNET OF THINGS JOURNAL, the IEEE TRANSACTIONS ON ANTENNAS AND PROPAGATION, the IEEE ANTENNAS AND WIRELESS PROPAGATION LETTERS, and *IET Microwaves, Antennas and Propagation*.



MANOS M. TENTZERIS (Fellow, IEEE) received the Diploma degree (*magna cum laude*) in electrical and computer engineering from the National Technical University of Athens, Athens, Greece, and the M.S. and Ph.D. degrees in electrical engineering and computer science from the University of Michigan, Ann Arbor, MI, USA. He was the Head of the GTECE Electromagnetics Technical Interest Group, the Georgia Electronic Design Center Associate Director of RFID/sensors

research, the Georgia Institute of Technology NSF-Packaging Research Center Associate Director of RF research, and the RF Alliance Leader. He is currently Ken Byers Professor of flexible electronics with the School of Electrical and Computer Engineering, Georgia Institute of Technology, Atlanta, GA, USA, where he heads the ATHENA Research Group (20 researchers). He has helped to develop academic programs in 3-D/inkjet-printed RF electronics and modules, exible electronics, origami and morphing electromagnetics, highly integrated/multilayer packaging for RF and wireless applications using ceramic and organic exible materials, paper-based RFID's and sensors, wireless sensors and biosensors, wearable electronics, Green electronics, energy harvesting and wireless power transfer, nanotechnology applications in RF, microwave MEMs, and SOP-integrated such as UWB, multiband, mm-wave, and conformal antennas. He was a Visiting Professor with the Technical University of Munich, Munich, Germany, in 2002, GTRI-Ireland, Athlone, Ireland, in 2009, and LAAS-CNRS, Toulouse, France, in 2010. He has authored more than 650 articles in refereed journals and conference proceedings, five books, and 25 book chapters. He has given more than 100 invited talks to various universities and companies all over the world. He is a member of the URSI-Commission D and the MTT-15 Committee, an Associate Member of the European Microwave Association (EuMA), a Fellow of the Electromagnetic Academy, and a member of the Technical Chamber of Greece. He was a recipient/co-recipient of the 2019 Humboldt Research Prize, the 2017 Georgia Institute of Technology Outstanding Achievement in Research Program Development Award, the 2016 Bell Labs Award Competition 3rd Prize, the 2015 IET Microwaves, Antennas, and Propagation Premium Award, the 2014 Georgia Institute of Technology ECE Distinguished Faculty Achievement Award, the 2014 IEEE RFID-TA Best Student Paper Award, the 2013 IET Microwaves, Antennas and Propagation Premium Award, the 2012 FiDiPro Award, Finland, the iCMG Architecture Award of Excellence, the 2010 IEEE Antennas and Propagation Society Piergiorgio L. E. Uslenghi Letters Prize Paper Award, the 2011 International Workshop on Structural Health Monitoring Best Student Paper Award, the 2010 Georgia Institute of Technology Senior Faculty Outstanding Undergraduate Research Mentor Award, the 2009 IEEE Transactions on Components And Packaging Technologies Best Paper Award, the 2009 E. T. S. Walton Award from the Irish Science Foundation, the 2007 IEEE AP-S Symposium Best Student Paper Award, the 2007 IEEE MTT-S IMS Third Best Student Paper Award, the 2007 ISAP 2007 Poster Presentation Award, the 2006 IEEE MTT-S Outstanding Young Engineer Award, the 2006 Asia-Pacific Microwave Conference Award, the 2004 IEEE Transactions on Advanced Packaging Commendable Paper Award, the 2003 NASA Godfrey Art Anzic Collaborative Distinguished Publication Award, the 2003 IBC International Educator of the Year Award, the 2003 IEEE CPMT Outstanding Young Engineer Award, the 2002 International Conference on Microwave and Millimeter-Wave Technology Best Paper Award, Beijing, China, the 2002 Georgia Institute of Technology–ECE Outstanding Junior Faculty Award, the 2001 ACES Conference Best Paper Award, the 2000 NSF CAREER Award, and the 1997 Best Paper Award of the International Hybrid Microelectronics and Packaging Society. He was the TPC Chair of the IEEE MTT-S IMS 2008 Symposium and the Chair of the 2005 IEEE CEM-TD Workshop. He is the Vice-Chair of the RF Technical Committee (TC16) of the IEEE CPMT Society. He is the Founder and the Chair of the RFID Technical Committee (TC24) of the IEEE MTT-S and the Secretary/Treasurer of the IEEE C-RFID. He is an Associate Editor of the IEEE TRANSACTIONS ON MICROWAVE THEORY AND TECHNIQUES, the IEEE TRANSACTIONS ON ADVANCED PACKAGING, and the *International Journal on Antennas and Propagation*. He served as one of the IEEE MTT-S Distinguished Microwave Lecturers, from 2010 to 2012, and one of the IEEE CRFID Distinguished Lecturers.



WENJING SU (Member, IEEE) received the B.S. degree in electrical engineering from the Beijing Institute of Technology, Beijing, China, in 2013, and the Ph.D. degree in electrical and computer engineering from the Georgia Institute of Technology, Atlanta, GA, USA, in 2018. In Fall 2013, she joined the ATHENA Research Group, led by Dr. MANOS M. TENTZERIS. She is currently working with Google LLC, Mountain View, CA, USA. She has authored over 37 articles in refereed

journals and conference proceedings. She holds four patents/patent applications. Her research interfaces advance novel fabrication technique, such as inkjet-printing and 3D printing, special mechanical structures, such as microfluidics and origami, and microwave components/antennas to solve problems in smart health, wearable electronics in the Internet-of-Things (IoT) applications. Her research interests include wearable antennas, flexible electronics, applied electromagnetics, additively manufactured electronics, wireless sensing, machine-learning aid sensing, green electronics, RFID, and reconfigurable antennas.